



## Field-scale demonstration of *in situ* immobilization of heavy metals by injecting iron oxide nanoparticle adsorption barriers in groundwater

Sadjad Mohammadian<sup>a</sup>, Beate Krok<sup>a</sup>, Andreas Fritzsche<sup>b</sup>, Carlo Bianco<sup>c</sup>, Tiziana Tosco<sup>c</sup>, Ekain Cagigal<sup>d</sup>, Bruno Mata<sup>e,1</sup>, Veronica Gonzalez<sup>f</sup>, Maria Diez-Ortiz<sup>f</sup>, Vanesa Ramos<sup>g</sup>, Daniela Montalvo<sup>h</sup>, Erik Smolders<sup>h</sup>, Rajandrea Sethi<sup>c</sup>, Rainer U. Meckenstock<sup>a,\*</sup>

<sup>a</sup> Environmental Microbiology and Biotechnology, University Duisburg-Essen, Universitätsstr. 5, 45141 Essen, Germany

<sup>b</sup> Institute of Geosciences, Friedrich Schiller University Jena, Burgweg 11, 07749 Jena, Germany

<sup>c</sup> Department of Environmental, Land and Infrastructure Engineering, Politecnico di Torino, Corso Duca degli Abruzzi, 24, 10129 Turin, Italy

<sup>d</sup> TECNALIA, Basque Research and Technology Alliance (BRTA), Parque Científico y Tecnológico de Bizkaia, Astondo bidea, Edificio 700, 48160 Derio (Bizkaia), Spain

<sup>e</sup> Geoplano Consultores, S.A, Zona Industrial de Casais da Serra, Lote 10, 2665-305 Mafra, Portugal

<sup>f</sup> LEITAT Technological Center, Carrer de Pallars, 179-185, 08005 Barcelona, Spain

<sup>g</sup> Knowledge Innovation Market – KIM, Carrer de Pallars, 179-185, 08005 Barcelona, Spain

<sup>h</sup> Division of Soil and Water Management, KU Leuven, Kasteelpark Arenberg 20, 3001 Leuven, Belgium

### ARTICLE INFO

#### Keywords:

Nanoremediation  
Heavy metals  
Iron oxide nanoparticles  
In situ remediation  
Permeable barriers  
Contaminated aquifer

### ABSTRACT

Remediation of heavy metal-contaminated aquifers is a challenging process because they cannot be degraded by microorganisms. Together with the usually limited effectiveness of technologies applied today for treatment of heavy metal contaminated groundwater, this creates a need for new remediation technologies. We therefore developed a new treatment, in which permeable adsorption barriers are established *in situ* in aquifers by the injection of colloidal iron oxides. These adsorption barriers aim at the immobilization of heavy metals in aquifers groundwater, which was assessed in a large-scale field study in a brownfield site.

Colloidal iron oxide (goethite) nanoparticles were used to install an *in situ* adsorption barrier in a very heterogeneous, contaminated aquifer of a brownfield in Asturias, Spain. The groundwater contained high concentrations of heavy metals with up to 25 mg/L zinc, 1.3 mg/L lead, 40 mg/L copper, 0.1 mg/L nickel and other minor heavy metal pollutants below 1 mg/L. High amounts of zinc (>900 mg/kg), lead (>2000 mg/kg), nickel (>190 mg/kg) were also present in the sediment. Ca. 1500 kg of goethite nanoparticles of  $461 \pm 266$  nm diameter were injected at low pressure (< 0.6 bar) into the aquifer through nine screened injection wells. For each injection well, a radius of influence of at least 2.5 m was achieved within 8 h, creating an *in situ* barrier of  $22 \times 3 \times 9$  m.

Despite the extremely high heavy metal contamination and the strong heterogeneity of the aquifer, successful immobilization of contaminants was observed in the tested area. The contaminant concentrations were strongly reduced immediately after the injection and the abatement of the heavy metals continued for a total post-injection monitoring period of 189 days. The iron oxide particles were found to adsorb heavy metals even at pH-values between 4 and 6, where low adsorption would have been expected. The study demonstrated the applicability of iron oxide nanoparticles for installing adsorption barriers for containment of heavy metals in contaminated groundwater under real conditions.

### 1. Introduction

Heavy metals and metalloid contaminations such as Zn, As, Pb, Cu

are of particular importance for groundwater resources since their high toxicity can cause diseases even at low concentrations (Marcovecchio et al., 2007). However, heavy metal ions are non-degradable and thus

*Abbreviations:* IW, Injection well; MCW, Multichannel well.

\* Corresponding author at: Prosolos, environment – 2625-437 Lisbon, Portugal.

*E-mail address:* [Rainer.Meckenstock@uni-due.de](mailto:Rainer.Meckenstock@uni-due.de) (R.U. Meckenstock).

<sup>1</sup> Current address: Prosolos, environment – 2625-437 Lisbon, Portugal.

<https://doi.org/10.1016/j.jconhyd.2020.103741>

Received 21 July 2020; Received in revised form 11 October 2020; Accepted 15 November 2020

Available online 28 November 2020

0169-7722/© 2020 The Author(s). Published by Elsevier B.V. This is an open access article under the CC BY license (<http://creativecommons.org/licenses/by/4.0/>).

very persistent and mobile in the environment posing severe threats for both ecosystems and human health.

Besides locally enhanced concentrations from geogenic sources, heavy metals are extensively released into the environment as a result of industrial activities such as plating, ceramics and glass production, mining and battery manufacturing, as well as from fertilizers for agricultural purposes and accidental oil spills from tankers (Uwamariya, 2013). Hence, heavy metals and metalloids are present in groundwater and soil of a significant number of contaminated sites. According to a report by the European Commission, more than 30% of around 2.8 million potentially contaminated sites across Europe contain heavy metals as main pollutants in both soil and groundwater (Paya Perez and Rodríguez Eugenio, 2018). However, up until 2015 only ca. 58,000 of these contaminated sites were remediated.

The most applied technology for the removal of heavy metals from groundwater is Pump & Treat where contaminated groundwater is pumped into above-ground installations and treated by either chemical precipitation, or reverse osmosis, adsorption, ion exchange, or electrochemical deposition. The clean water is commonly reinjected into the ground (Al-Saad et al., 2012; Barakat, 2011) or discharged in sewage systems or surface water bodies, depending on national legislative frameworks and residual contamination levels after treatments. Typically, the Pump & Treat method requires the installation of large facilities on site and investments or operation costs in the Million-Euro range, which are limiting factors for remediation efforts. Hence, in many cases in-depth remediation is economically not feasible due to e.g. low concentrations of contaminants, location in urban or sealed areas prohibiting constructions or installations for water treatments, or limited financial resources of the responsible for clean-up.

Here, we demonstrate a new technology to mitigate the spreading of heavy metal contaminations by installing an *in situ* permeable adsorption barrier using iron oxide nanoparticles (Braunschweig et al., 2013; Khin et al., 2012; Saha et al., 2013; Skjolding et al., 2016). The concept includes that colloidal nanoparticles can be introduced into aquifers through injection wells, where, due to their minute size, they can spread in the subsurface with the pumped water. Once they reached the target radius of influence, they should aggregate and subsequently deposit at the surface of the aquifer matrix.

Iron oxides are naturally present in aquifers, have low toxicity, and pose no danger to the environment or the operators (Cabellos et al., 2018; González-Andrés et al., 2017). Moreover iron oxide nanoparticles offer larger surface areas in comparison to bulk iron oxide, which in turn increases the adsorption sites for heavy metals (Waychunas et al., 2005). Unlike other iron-based nanomaterials, such as nano-zerovalent iron (nZVI) (Saleh et al., 2006; Tiraferrri et al., 2008; Tosco et al., 2014), iron oxide nanoparticles can remain colloidal in the injection fluids. Consequently, they form stable suspensions and do not clog the pores of the aquifer matrix during injection due to coagulation or corrosion, which allows for injection at low pressure thus avoiding a potential fracturing of the underground. Contact with electrolytes, e.g. groundwater, induces the aggregation of the iron oxide colloids, which can be exploited to specifically tune the propagation of the colloids through the aquifer during their injection (Bianco et al., 2017; Tiraferrri et al., 2017; Tosco et al., 2012). Their finite and controllable mobility and their gentle injection makes colloidal iron oxides particularly suitable for groundwater remediation at field-scale.

Iron oxides and in particular goethite ( $\alpha$ -FeOOH) are known to adsorb many metal(loid)s such as arsenate,  $Zn^{2+}$ ,  $Pb^{2+}$ ,  $Cu^{2+}$ , and others from contaminated water (Abdus-Salam and Adekola, 2005; Mohapatra et al., 2010; Montalvo and Smolders, 2019; Rodda et al., 1993). The affinity of goethite towards heavy metals is pH-dependent (Abdus-Salam and Adekola, 2005; Al-Saad et al., 2012; Montalvo and Smolders, 2019) and is strongest at neutral to slightly alkaline pH-values. At neutral pH-values, heavy metals still dissolve in water and are transported with groundwater, but also strongly adsorb to goethite nanoparticles. In contrast, the electrostatic attraction between goethite and metal ions

decreases at acidic pH, while the solubility of metal ions decreases at strong alkaline conditions.

This study presents a field test of injecting colloidal iron oxides for the installation of an *in situ* adsorption barrier for immobilizing heavy metals in contaminated groundwater. The objectives of the study were (i) to evaluate the use of goethite colloids for implementing a stable and permeable *in situ* adsorption barrier for heavy metals; and (ii) to determine the efficiency of these nanoparticles in removing mobile heavy metal contamination from groundwater.

## 2. Methodology

### 2.1. Site description

The Nitrastur site is an abandoned 20 ha flat brownfield, located near Langreo, Asturias, Northern Spain. Historically, it was used over 48 years (1950–1998) for the production of nitrogen-based products, such as fertilizers. The whole site area is covered by a layer of madeground (177,000 m<sup>2</sup>), with a variable thickness between 2 m and 9 m. The madeground materials include slag from furnaces, wastes from coal-washing and partially burned pyrites, pyrite ashes – which are typically rich in heavy metals – as well as construction debris. Underneath the madeground, there is a 3–6 m thick layer of quaternary alluvial deposits of sandy, silty gravels with boulders which define the unconfined and porous aquifer of the site. Beneath the aquifer, there is a less permeable, very hard slate and sandstone layer from the Carboniferous, acting as an aquitard (Wcisto et al., 2016). The groundwater level is located close to the contact area between the madeground and the alluvial materials, ca. 2–3 m below the surface (Fig. 1). The groundwater flows with an average velocity of 1.1 m/day towards an adjacent perennial river.

The main source of contamination on the site is the madeground (Fedje et al., 2017; Wcisto et al., 2016); its high levels of heavy metals from the pyrite ashes leach into the groundwater and become mobilized by rainwater seepage and groundwater fluctuation. According to Gallego et al. (2016), who performed a sequential extraction of the madeground, Zn, Pb, and Cu are the most mobile heavy metals leaching into the underlying aquifer (Gallego et al., 2016; Wcisto et al., 2016). In the test area, the electrical conductivity was relatively low (923–2670  $\mu$ S/cm) and the oxidation-reduction potential of about +400 mV indicated oxic conditions.

### 2.2. Installation of the barrier

The technology demonstration was conducted in a ca. 22 m  $\times$  35 m area of the site, where the thickness of the madeground layer was the lowest (2–3 m). The adsorption barrier was installed with nine injection wells that were placed in two lines perpendicular to the groundwater flow direction, to maximize the efficiency (Fig. 2a, b). The distance between the injection wells was 4 m, allowing an overlap of one meter considering a radius of influence of 2.5 m for each well. The injection wells had a diameter of 76 mm (3 in.) and were screened from ca. 1 m below the water table, at 3.5 m below surface, down to the bottom of the aquifer at 6.5 m below surface, to avoid intrusion of the iron oxides into the unsaturated zone (Fig. 2).

Furthermore, 11 regularly screened monitoring wells and 4 multi-channel wells (MCW) with 3 channels each were installed for groundwater monitoring (Fig. 2a and c). The multichannel wells provided vertical profiles of the heavy metal concentrations and the migration of the iron oxide colloids during the injection inside (MCW 1 and MCW 2) and downstream of the barrier (MCW3 and MCW4). Two upstream (P1 and P2) and nine downstream regular monitoring wells (P3–P11) were installed to assess the heavy metal removal by the adsorption barrier and to identify putative migration of colloids.

Slug tests using a cylindrical slug with a diameter of 2.5 cm and length of 100.0 cm were carried out in all nine injection wells before

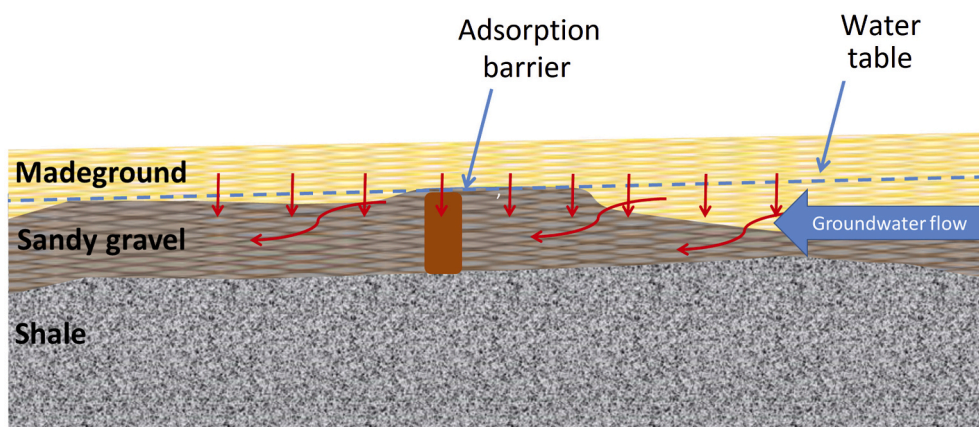


Fig. 1. Conceptual model of the Nistratur site in Northern Spain. The red arrows show the passage of heavy metals. (For interpretation of the references to colour in this figure legend, the reader is referred to the web version of this article.)

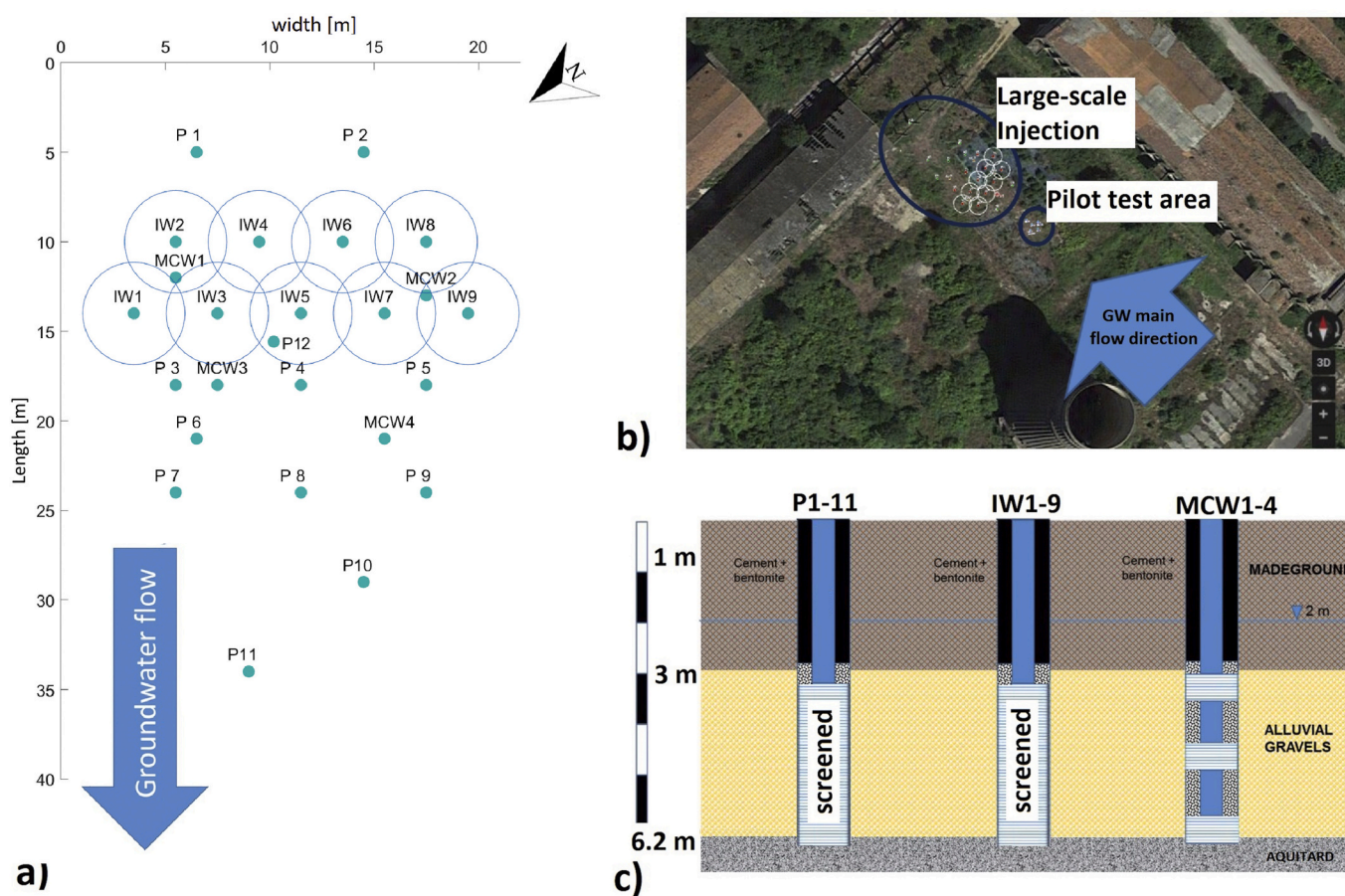


Fig. 2. Installation of the *in situ* adsorption barrier on the brownfield. a) Schematic top view of the injection wells, the groundwater monitoring wells and the expected adsorption barrier. Injection was carried out in IW1 on the first day, followed by IW5 and IW7 (second day), IW2 and IW4 (fourth day), and IW3 and IW9 (fifth day). The destabilizing agent was injected into P3, P4, and P5 on the third day. Well P12 was drilled after the injection of the nanoparticles and was used only for analysis of sediment. b) Location of the test area for implementing the *in situ* adsorption barrier. GW stands for groundwater. c) Schematic representation of the installed injection and monitoring wells. P1-11 depicts the schematic design of the monitoring wells P1 through P11, IW1-9 of injection wells IW1 through IW9, and MCW of multi-level monitoring wells MCW1 through 4.

installing the adsorption barrier. The hydraulic conductivity of the aquifer was found to be  $5.08 \pm 4.53 \times 10^{-4}$  m/s. During a pilot study on the site (data not shown) it was found that the conductivity of the aquifer varies strongly with depth, showing a highly permeable layer in the bottom part of the aquifer, and less conductive materials in the upper part, close to the madeground. The existence of a higher conductivity

layer at the bottom of the aquifer was also confirmed by the monitoring data registered during our iron oxide injection (see below). A faster breakthrough of the colloid suspension was observed already after 1 h in the deepest sampling ports of MCW1 and MCW2 at 6 m – 6.3 m depths compared to the two upper ports, although it was expected after 5 h.

### 2.3. Production and injection of the iron oxide nanoparticles

The suspensions of colloidal goethite were synthesized and coated with humic acids at the University of Duisburg-Essen according to Meckenstock and Bosch (2014). These humic acid-coated goethite colloids have been previously shown to successfully immobilize heavy metals in laboratory experiments (Montalvo and Smolders, 2019; Montalvo et al., 2018) and to be mobile in similar porous media (Bianco et al., 2017; Tiraferri et al., 2017). The colloid suspension was produced with a goethite content of ca. 100 g/L, a humic acid content of 6 g/L for stabilization of the suspended particles, and a pH of 9–10 and remained stably colloidal during storage in 1200 L Intermediate Bulk Containers (IBCs) for several months. However, for the present study, the 15 m<sup>3</sup> suspension was freshly produced and shipped to the site within one week from production.

The colloid suspension was analyzed with X-ray diffraction and Fourier-transform infrared spectroscopy, which revealed that the nanoparticles consisted solely of low-crystalline goethite (see supplementary materials S1 to S3). The hydrodynamic diameters of the colloids were measured with dynamic light scattering (Nano ZS, Malvern Instruments), revealing an average size of  $d_H = 461 \pm 266$  nm. N<sub>2</sub>-physisorption (Autosorb 1; Quantachrome) was evaluated with BET isotherms and revealed an average specific surface area of  $161.0 \pm 0.2$  m<sup>2</sup>/g (min/max-deviation from duplicate analysis).

On the site, the colloids were diluted 1:10 with municipal water and injected with packers into the injection wells at a flowrate of ca.  $30 \pm 6$  L/min. Prior to each injection, ca. 1 m<sup>3</sup> of water was injected into each well in order to reduce the direct contact between groundwater and the iron oxide suspension, which would trigger aggregation and thus deposition of the colloids (Bianco et al., 2017). Considering the relatively shallow water table, we injected only into two parallel wells per day to avoid a strong increase of the groundwater table and possible daylighting. The injection pressure in each well was monitored continuously above the packer at the surface in order to detect possible pore clogging or fracturing.

During, before and after injection, groundwater samples (200 mL each) were collected from 24 wells: 11 monitoring wells (P1-11), 9 injection wells (IW1-9), and 4 multichannel wells (MCW1-4). In addition, soil samples from well IW5 were analyzed to determine the iron content of the sediment in various depths. An additional well (P12) was drilled ca. two months after the application and the iron content was compared to the one before injection to determine the spreading and the deposition of the nanoparticles.

### 2.4. Analysis of groundwater

Heavy metal concentrations in the groundwater samples were analyzed with ICP-MS (X-Series II, ThermoFisher Scientific). Prior to analysis, the samples were treated with HCl (37%, AnalaR NORMAPUR; VWR Prolabo) and H<sub>2</sub>O<sub>2</sub> (30%, Rotipuran; Carl Roth GmbH + Co KG) to completely dissolve potentially occurring ferric oxide nanoparticles. In addition, the pH (Sentix 41; WTW) and electric conductivity (TetraCon 325; WTW) were measured in untreated groundwater samples.

The sediment samples from IW5 and P12 were dried (105 °C; ED 53; Binder), sieved (<2 mm) and grinded in a planetary mill (45 min; PM 100 CM; Retsch). Tablets were prepared with homogenized sediment samples and Hoechst wax C micropowder (Merck) in a 1:6 mass ratio and the samples analyzed using wavelength dispersive X-ray fluorescence (WDXRF; PW 2400; Philips). The iron content of the sediment samples was also determined according to the dithionite-citrate-bicarbonate extraction protocol (Mehra and Jackson, 1958) and served as indicator to trace the propagation of goethite nanoparticles after injection.

## 3. Results

### 3.1. Injection of the ferric oxide colloids for installation of the permeable adsorption barrier

The injection was started in IW1 on day 0. On the next day (day +1) the the suspension was injected in IW5 and IW7 simultaneously. At the end of this day, traces of brownish iron oxide fluid were observed in the downstream wells P3, P4, and P5 as well as in the deepest part of MCW3 (Fig. 3b and d), indicating the presence of a high conductivity layer at the lower part of the aquifer. In order to prevent downstream migration of the nanoparticles, the NanoTune approach developed at Politecnico di Torino was applied by equally injecting a total volume of ca. 26,700 L of a destabilizing agent (1 mM CaCl<sub>2</sub> in water, according to Tiraferri et al. (2017)) into P3, P4, and P5 (Bianco et al., 2017). The iron oxide injection was resumed on day +3 by injecting nanoparticles into IW2 and IW4, continued by IW6 and IW8 on day +4, and IW3 and IW9 on day +5. No visible traces of goethite colloids were found in the other downstream wells. Throughout the application, the injection pressure remained between 0.4 and 0.6 bars for all the wells and no daylighting occurred. The detailed properties of the suspension are shown in Table S9 (supplementary materials). Within the first two weeks after the injection of the goethite nanoparticles, the pH in the wells returned to their pre-injection values with the exception of some of the wells located in the acidic area (IW2, IW3, IW4, IW5, P7, and P8), in which the pH varied between 3 and 7 in comparison to pre-injection values of 2–4 (Fig. S4a-b). The injection of the destabilizing agent did not alter the pH in the wells P3, P4, and P5. No significant increase in mobile organic carbon was observed (Fig. S8 supplementary materials) indicating that the humic acid was not released from the goethite nanoparticles during the monitoring period.

Slug tests were carried out in all the injection wells immediately (day +6) and ca. one year (day +325) after the injection. The measured values were  $2.63 \pm 0.76 \times 10^{-4}$  m/s and  $4.52 \pm 4.31 \times 10^{-4}$  m/s, respectively. The lower values immediately after the injection were presumably due to the presence of the still suspended particles in the wellbore. Nevertheless, the hydraulic conductivity of the aquifer returned to the pre-injection conditions ( $5.08 \pm 4.53 \times 10^{-4}$  m/s) and was not affected by the injection.

One week after the injection, the iron concentrations returned to their initial pre-injection values in all wells, indicating that the colloids were deposited at the matrix surfaces within less than one week after the injection and were not continuously exported from the barrier with the groundwater flow (Fig. 3). Two months after the injection, a sediment core was drilled 2 m away from IW5, at P12 in the central region of the barrier, to monitor the distribution of the iron oxides (Fig. 2a). Even at 2 m distance from the injection well, the iron content in the sediment was increased by, on average, 2000 mg/kg sediment compared to the background level of the neighboring sediment core taken during installation of well IW5 before the injection (Fig. 4). This increased iron content showed that the injected colloids did not precipitate only around the wellbore but were successfully delivered to the intended radius of influence of 2.5 m. An accumulation of iron oxides was specifically observed from 6 to 6.3 m depth where, most likely, more of the iron oxide colloids was delivered due to the highly conductive zone at the bottom of the aquifer.

### 3.2. Monitoring of water chemistry

Before the injection, analysis of groundwater samples revealed a strong heterogeneity of the pH in the test area. While water of most of the wells showed a neutral pH, some wells (P3, P4, P6 P7, IW2, IW3, IW4, and IW5) showed pH-values below 5, even reaching values down to pH 3 at some sampling times (Fig. 5). This acidic area was partially buffered by the injection solution of the ferric oxide colloids (pH ~ 9.5), but the original pH-values recovered in all wells shortly (less than one

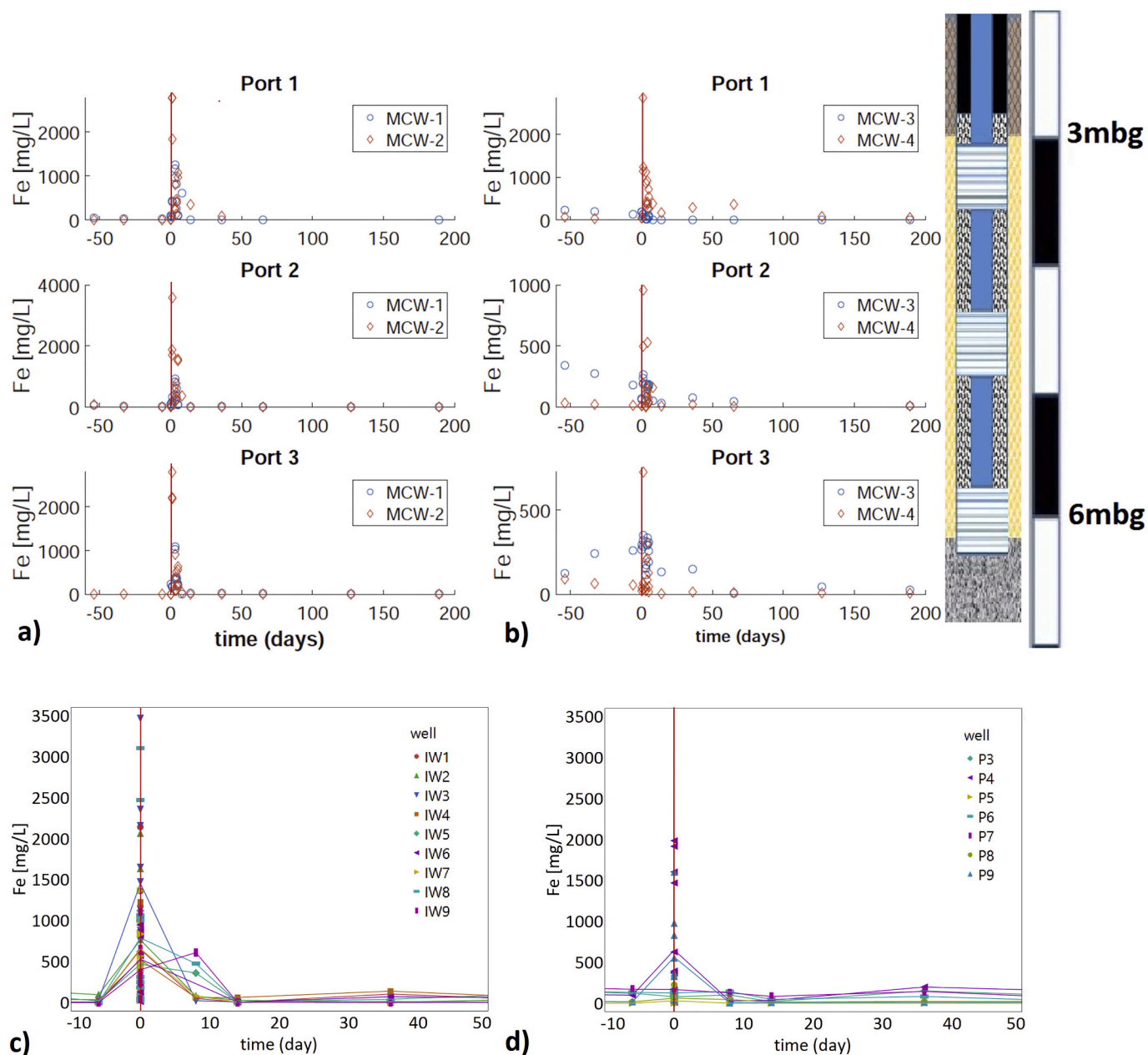


**Fig. 3.** Observed iron concentrations in water samples of the multichannel wells MCW1 to MCW4 (a, b), injection wells (c), and the first two rows of the downstream monitoring wells (d) as indicator for the mobility or precipitation of the goethite colloids. Day 0 (the red vertical line) indicates the first day of the injection. The schematic drawing of the multi-channel well indicates the filter zones at different depths. Mbg: meters below ground. (For interpretation of the references to colour in this figure legend, the reader is referred to the web version of this article.)

week) after the injection (Supplementary info S4a-b).

Prior to the injection of the iron oxide colloids, high heavy metal concentrations in the groundwater were around  $25 \pm 17$  mg/L for Zn,  $40 \pm 25$  mg/L for Cu, and  $1.3 \pm 2.5$  mg/L for Pb (Fig. 5). The highest concentrations were found inside the acidic area, e.g. in P3, P4, P6, and P7, IW2, IW3, and IW5, where heavy metal concentrations were found to be ca. ten times higher than in the rest of the wells.

Analysis of the sediment profile, obtained from cores of IW5, showed that high amounts of heavy metals were present not only in the made-ground (0–3 m below surface), but also in all depths of the aquifer materials (Fig. 6). The total metal content of the aquifer sediment was higher than 1500 mg/kg in all depths, reaching 7320 mg/kg just below the groundwater table.

### 3.3. Immobilization of heavy metals by the adsorption barrier

Right after the injection on day 0, the heavy metal concentrations of Zn, Cu, and Pb sharply decreased in all wells (Fig. 7a-f, full data set in supplementary Fig. S5a-e). Except for a few data points, the heavy metal concentrations remained below 50% of the background values, even for the wells located in the acidic area. The concentrations of the dominant pollutants Zn and Cu were reduced from more than 25 mg/L to below 3 mg/L. In some wells (e.g. P6) more than 90% of the heavy metals were immobilized from the groundwater. The immobilization of the heavy metals continued throughout the monitoring period of 189 days after the injection.

In the post-injection sampling on days +35 and +189, an increase of Zn, Cu, and Pb concentrations was observed in all wells, notably in the acidic area (P3, P4, P6, IW3, IW4, IW5, Fig. 7a-f). This increase is

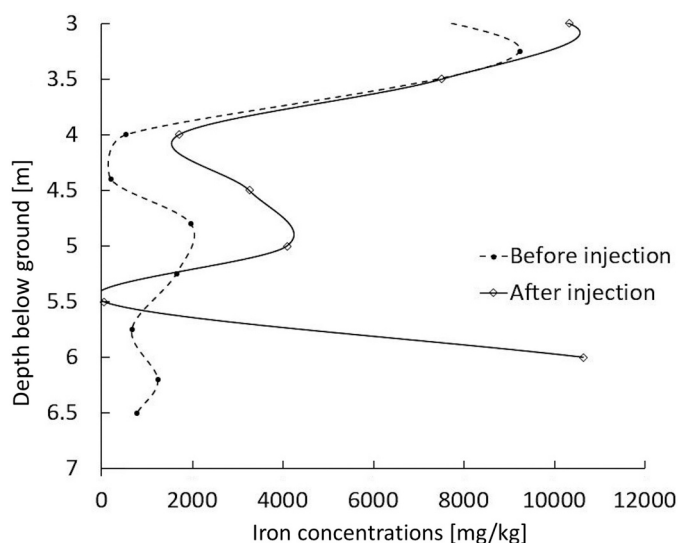


Fig. 4. Comparison of the iron content in the sediment before (core taken at IW5, Fig. 2a) and after injection of the nanoparticles (core taken at P12, Fig. 2a).

attributed to leaching from the madeground layer into the aquifer as a consequence of rain events (Supplementary material, Fig. S6). For example, in the weeks of the last sampling date (day +189) a total precipitation of more than 120 L/m<sup>2</sup> was recorded in the nearby meteorological station. The leached heavy metals are more mobile in low pH conditions; hence the effect is pronounced in the wells located in the acidic area.

### 3.4. Adsorption of heavy metals

We estimated the efficiency of the barrier by calculating the contaminant flux and the adsorption for the injection wells. The cross section area of the installed barrier was ca. 22 m × 3 m perpendicular to the groundwater flow. In each injection well, 16.5 ± 0.7 m<sup>3</sup> colloid suspension were injected with an iron oxide concentration of ca. 10 kg/m<sup>3</sup>. Hence, on average ca. 22.5 kg of goethite was delivered to each cross section unit area of 1 m<sup>2</sup>. Previous studies (Montalvo and Smolders, 2019) found that, under favorable conditions (pH 6.1 to 7.0), the adsorption capacities of the present goethite colloids in a multi-element system similar to the groundwater are 9 g/kg<sub>nanoparticles</sub> for Zn and 51 g/kg<sub>nanoparticles</sub> for Cu. Therefore, the injected amount of iron oxides is expected to adsorb 202.5 g Zn and 1147.5 g Cu per unit cross section area of 1 m<sup>2</sup>. Considering average concentrations of 25 mg Zn/L and 40 mg Cu/L in groundwater of the wells in the acidic area (e.g. IW2 or IW3), a porosity of 25%, and a groundwater flow velocity of 1.1 m/day, the groundwater transported a mass of ca. 6.9 g Zn and ca. 11 g Cu per day across a unit cross section area. This means that the amount of injected goethite is expected to become saturated in about 29 days for Zn and 104 days for Cu. Nevertheless, the concentrations of mobile Zn and Cu remained below 1 mg/L in IW2 and IW3 until +128 days after the injection (Fig. 7d-e). The apparently enhanced longevity of the installed barrier could be partially explained by the pH changes in the injection area. The pH values of the samples collected from some of the wells inside the acidic area (IW2, IW3, IW4, IW5, P7, and P8) were increased from 2 to 3 to 3–7 (Fig. S4a-b). It is known that the mobility of metals decreases at alkaline pHs (Chuan et al., 1996; Król et al., 2020). However this trend was not observed for all the wells, especially for those outside the acidic area. The post-injection pH values remained neutral to slightly acidic throughout the monitoring period. Nevertheless, reduction in heavy metal concentrations was observed both inside and outside the acidic area. Reduction in metal concentrations was observed across

the pH values, even in P3 and P7, where the pH values remained below 4 after the injection. Additionally, seepage water from rainfall events introduced unknown amount of heavy metals from the madeground layer into the aquifer, causing fluctuations in incoming metal fluxes. Such fluctuations are also observed in the pre-injection data. Changes in groundwater velocity, and presence of other iron minerals in the sediment may have influenced the longevity of the installed barrier, too. In the following 2–3 months the concentrations increased only in the acidic area, where the injected goethite nanoparticles became saturated. In all other wells, where initial concentrations were lower, a continuous decrease in heavy metal concentrations was recorded throughout the monitoring period after injection (189 days).

## 4. Discussion

Heavy metal contamination of groundwater is a world-wide problem, but only few technologies are available for its remediation. The most applied Pump and Treat technology has considerable disadvantages, such as ineffectiveness at lower heavy metal concentrations or its high costs (Dolgormaa et al., 2018). Since financial limitations constitute a major drawback for remediation, there is a strong demand for *in situ* technologies that are cheaper and easier to implement (Karn et al., 2009; Perelo, 2010). We therefore conducted a demonstration scale experiment to install an *in situ* adsorption barrier based on colloidal iron-oxides that can be injected into aquifers.

The concept of the *in situ* adsorption barrier for heavy metals is based on three pillars. First, the injected iron oxide nanoparticles must be perfectly colloidal since they have to travel over several meters in the aquifer without clogging the pore space. Second, the particles must be metastable, that is they must precipitate shortly after the injection and cover the sediment to become immobile so the *in situ* adsorption barrier stays at the point of injection and particles do not dislocate with the groundwater flow. Third, the iron oxides have to adsorb the heavy metals in the groundwater below the remediation targets.

The colloidal goethite used in this study was proven to be ideally injectable into the aquifer. The constantly low pressure throughout the injection confirmed that the colloidal iron oxides in the suspension did not agglomerate and did not clog the pores around the wellbores. This observation was confirmed by measuring the same hydraulic conductivity of the aquifer with slug tests before and after the injection.

The mobility of the goethite nanoparticles is thus superior compared to other nanomaterials such as nanoscale Zero Valent Iron (nZVI), which tends to aggregate and block the pores (EPA, 2009; Kocur et al., 2014; Phenrat et al., 2007). Hence, high pressure is required to push nZVI into the sediment (He et al., 2010), which may lead to fracturing of the aquifer and thus uncontrolled and inhomogeneous spreading of the particles. In contrast, the goethite nanoparticles were effectively transported over the intended radius of influence, which exceeded 2.5 m at low pressure (<1 bar). This was confirmed by elevated iron concentrations in the groundwater samples taken from MCW-1 and MCW-2 during the injection, which are located inside the barrier region (Figs. 3c-d and S7a-b). Iron concentrations were increased only in days +3 and +1, respectively, which were the exact days that goethite nanoparticles were injected into the nearby wells of IW2 and IW9, respectively.

However, the injected goethite nanoparticles were clearly metastable and aggregated shortly after the injection was finished and were deposited at the matrix surfaces, which is a prerequisite to establish a stationary *in situ* permeable barrier. Reduction in mobile iron concentrations shortly after injection indicated that the injected goethite nanoparticles were immobilized (Fig. 3c and S7a-b). The successful delivery of the nanoparticles was verified by the elevated iron content in the sediments 2 m away from the injection point, proving that the injected particles were indeed deposited in the barrier region, i.e. they neither accumulated near wellbores nor were transported with the groundwater. The elevated iron content shown in Fig. 4 is between 900 and 2100 mg/kg in depth between 4 and 5 m below surface. This value

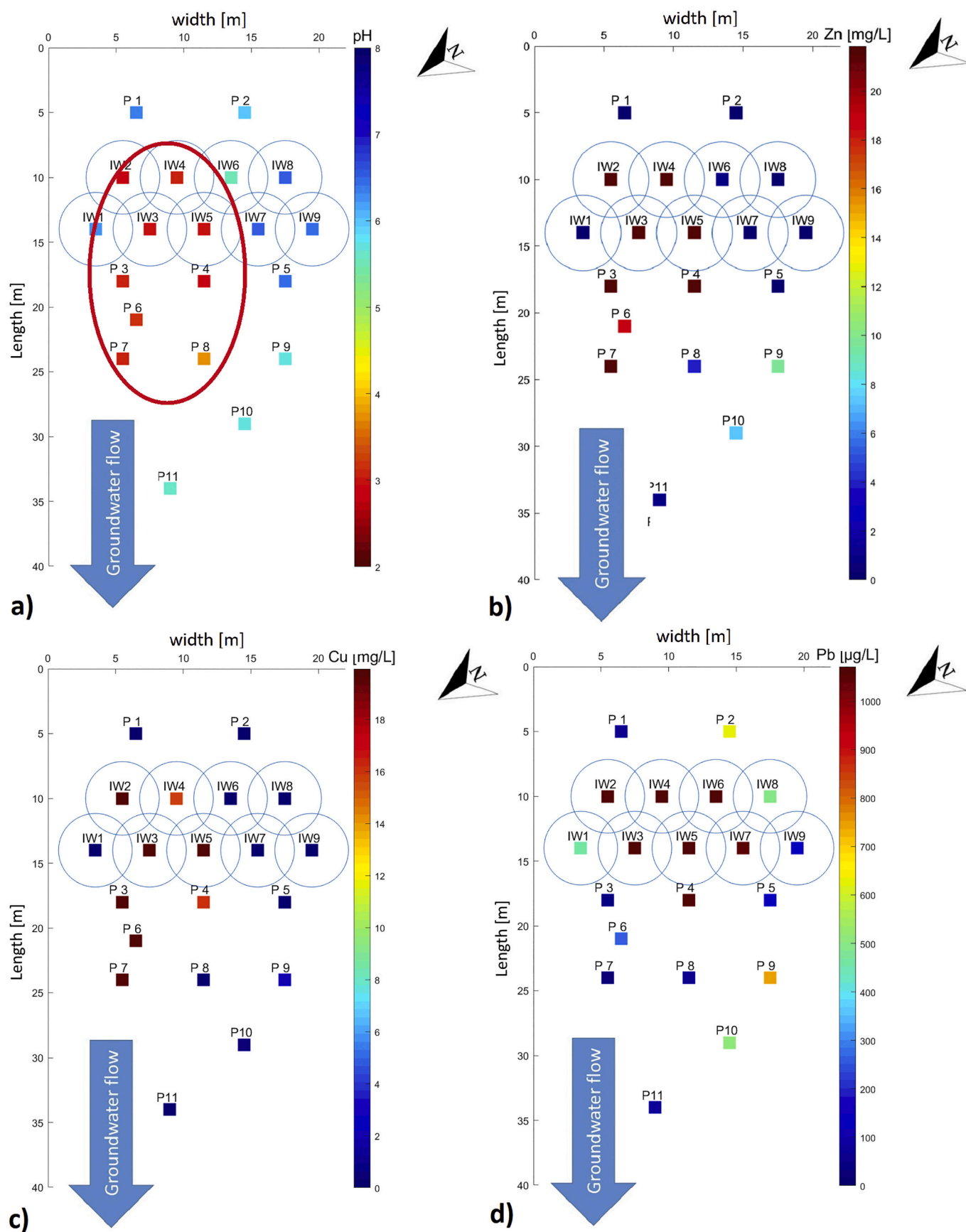


Fig. 5. Heterogeneity of pH-values and heavy metal concentrations in the test area at 33 days before injection. The colors indicate pH-values or heavy metal concentrations measured in each well according to the depicted color scales. Panel a) pH values in the test area, b) Zn, c) Cu, and d) Pb concentrations. The acidic

area is shown inside the red ellipse in panel a. (For interpretation of the references to colour in this figure legend, the reader is referred to the web version of this article.)

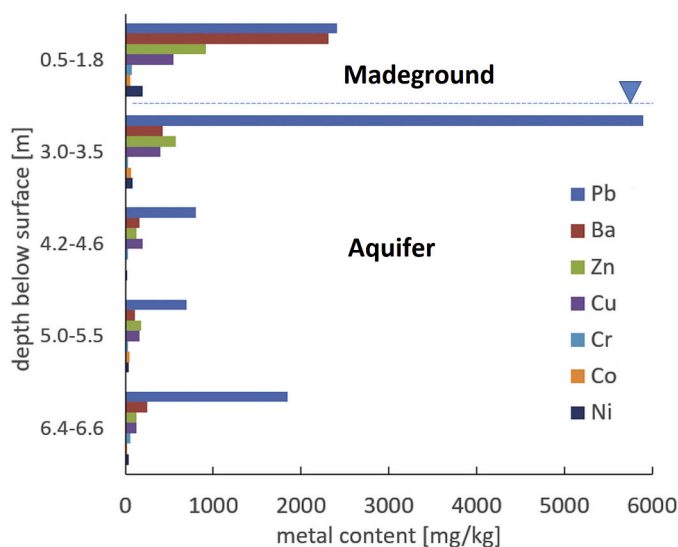


Fig. 6. Depths distribution of the most abundant heavy metals in a sediment core taken at IW 5 before injection of the barrier. The dashed line and the triangle indicate the groundwater table.

matches the expected increase in iron content due to injection of ca. 10 kg/m<sup>3</sup> of goethite nanoparticles. At deeper zones, however, the observed iron concentrations exceeded the expected amount. This is probably due to preferential flow of the injected goethite nanoparticle suspension into the highly conductive zone at the bottom of the aquifer. Very high iron content in this zone is hence attributed to accumulation of the goethite nanoparticles from the adjacent depth (e.g. 5 to 6 m). This observation is in agreement with a three dimensional injection study (Velimirovic et al., 2020), where the delivery and the fate of similar goethite nanoparticles were observed and modelled. In both, the study by Velimirovic et al. (2020) and the present study, goethite colloids became immobile shortly after the injection ended, forming a stable *in situ* barrier of the intended radius of influence. Similar to the present study, Velimirovic et al. (2020) also observed preferential migration of the injected colloids in a highly conductive zone and, hence, deposition of the colloids according to the distribution of the hydraulic conductivity of the aquifer. Although this inhomogeneity seems to be a disadvantage of the injection method, it is indeed favorable as more iron oxide is delivered to the regions through which the contaminated groundwater flows. Hence, the largest deposition of goethite particles is at the very place of the highest contaminant flux. This is highly desired since it provides an automated, passive regulation to deposit the adsorbent exactly where it is needed.

The third requirement is the effectiveness of the barrier. Iron oxides are excellent adsorbents for heavy metals in general (Al-Saad et al., 2012; Dolgormaa et al., 2018; Shen et al., 2020; Uwamariya, 2013), and our goethite colloids showed particularly effective adsorbance for the removal of heavy metals from groundwater (Montalvo and Smolders, 2019; Montalvo et al., 2018). Furthermore, the small size of the iron oxide colloids offers much higher surface area for adsorption of toxic metals in comparison to bulk iron oxides.

The analysis of the groundwater samples taken after the implementation of the adsorption barrier showed that the concentrations of the dissolved toxic metals such as Zn, Cu, and Pb were reduced during the post-injection monitoring period of 189 days. High inflow concentrations of heavy metals were observed from the madeground layer into the aquifer across the test area. Baragaño et al. (2020) conducted

controlled flooding experiments in an upstream well nearby the area of the pilot study (see Fig. 2b) and observed leaching of heavy metals from the madeground layer into the aquifer. Rainfall events and accordingly occurring seepage water transports unknown amounts of heavy metals from the madeground layer to the aquifer and, hence, affect the observations in the downstream monitoring wells. Despite continuous inflow of toxic metals from the overlaying madeground layer (especially on days +35 and +189 due to heavy rainfall) and low pH values in some parts of the tested area, which may lead to partial release of the metals, concentrations of the toxic metals remained below 50% of the background values, even at wells with pH values below 4 (e.g. P3 and P7), and in some cases more than 90% of the toxic metals were eliminated from the groundwater over our monitoring period of 189 days.

Although generally higher dissolved heavy metal concentrations were measured in the wells located in the acidic area, the goethite nanoparticles still reduced the concentrations significantly (Fig. 7). For example, the concentrations of Zn measured in monitoring well P7 within the acidic pH area decreased from ca. 45 mg/L to ca. 5 mg/L. This was somehow surprising since most metal cations adsorb to a lesser extent to iron oxides at pH values below 6.0 (Montalvo and Smolders, 2019; Okazaki et al., 1986). However, the adsorption capacity of the injected iron oxide must have been sufficiently high to overcome this limitation. At the same time, a reduction from 7 mg/L to <1 mg/L of Zn was observed in P10, which was located within the neutral pH area. Nevertheless, the amount of iron oxide nanoparticles required for a similar adsorption capacity in a barrier is potentially higher compared to an aquifer with neutral pH conditions (Montalvo and Smolders, 2019).

The current study also presents some projections about the long-term fate of the injected goethite nanoparticles and of the sorbed metals. Since no mobile iron was detected in the downstream monitoring wells and after the injection, one concludes that the injected goethite nanoparticles were bound to the sediment matrix. Hence, the risk of particle-bound transport of pollutants is negligible. Goethite is one of the most thermodynamically stable iron oxide minerals and dissolves at ambient conditions only at very low pH, at presence of iron-complexing compounds (e.g., oxalic acid) or under anoxic conditions, e.g. by reducing agents and/or anerobic microbial reduction (Schwertmann, 1991). Although a portion of the *in situ* adsorption barrier was located in an acidic area, no indication of iron dissolution was observed. Previous studies e.g. (Vermeer et al., 1999) showed that the addition of the humic acid can enhance the adsorption of heavy metals to iron oxides. The present study cannot distinguish between the adsorption of heavy metals to goethite or humic acid. Nevertheless, the negligible amount of humic acid released suggests that the transport of the toxic heavy metals with humic acid is not expected in long term. Rebound of adsorbed heavy metals from humic acid coated goethite may occur if the pH of groundwater drops significantly (Chuan et al., 1996; Violante et al., 2010), anoxic conditions evolve or strong Fe-complexing agents are introduced. The latter two scenarios can be excluded from the site properties and history. However, the reduction in the pH values correlates with the rainfall events and inflow of metal-rich leachate from the madeground layer, which, in longer monitoring times, leads to fluctuations in observed metal concentrations. Furthermore, competition among divalent cations for adsorption onto humic acid-coated goethite will eventually result in the release of heavy metals with lower affinities. Montalvo and Smolders (2019) observed that, as more adsorption sites became occupied with time, Cd and Ni were released from goethite nanoparticles and became replaced with Cu and Zn. Hence, under multielement contamination conditions remobilization of low affinity heavy metals might occur, and the competition of the present heavy metals for adsorption must be taken into account.

For designing an *in situ* adsorption barrier for plume treatment, it is



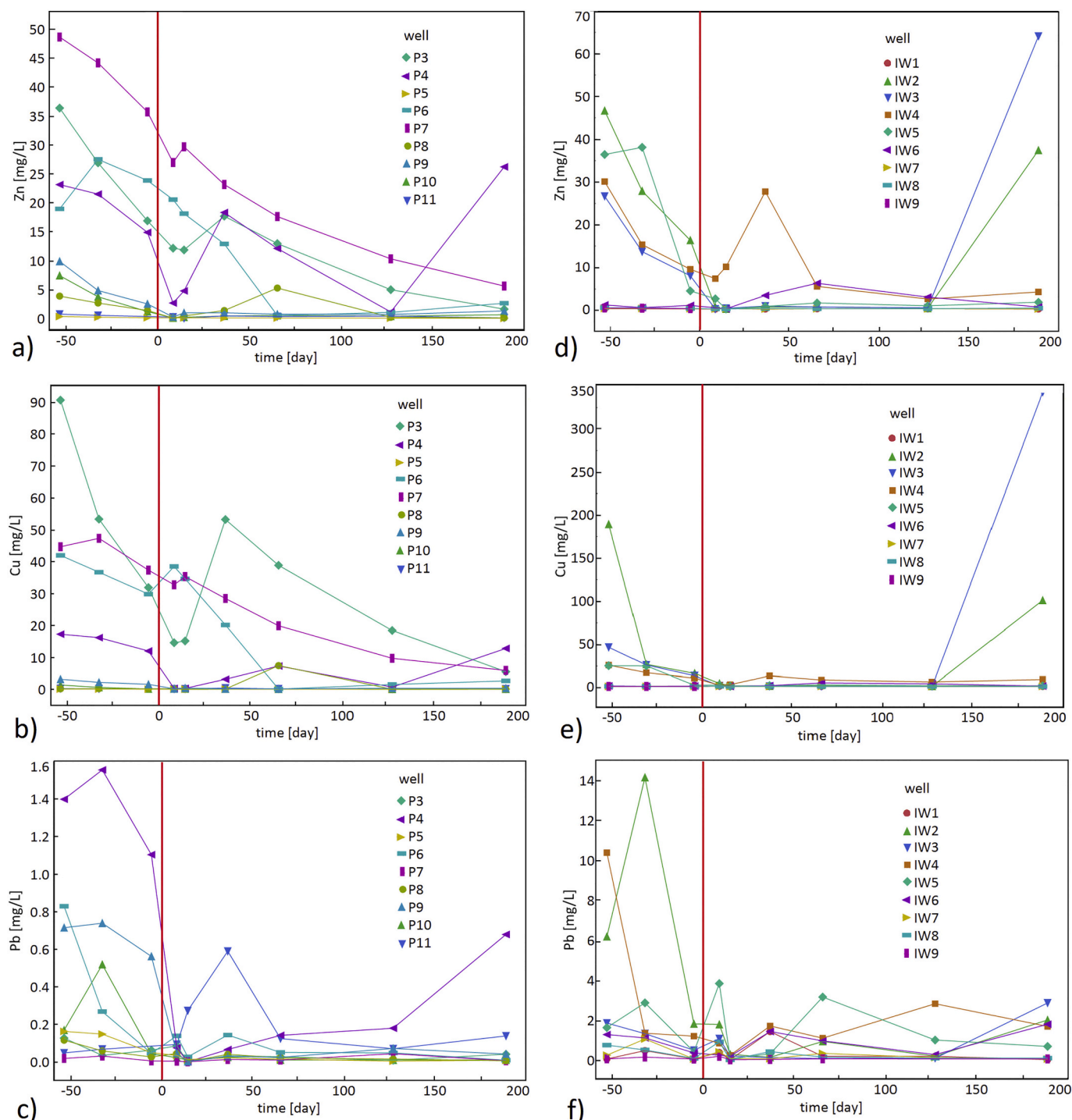


Fig. 7. a-f: Observed Zn, Cu, and Pb concentrations in monitoring downstream wells (a-c) and injection wells (d-f). Time 0, indicated by the red vertical line, indicates the day of the injection.

also important to consider the heavy metal content associated with the solid phase in the aquifer. In our case, the heavy metal content of the sediment accounted for several hundred mg/kg (Fig. 6). In chemical equilibrium, these sediment-associated heavy metals are constantly being released from and adsorbed to the sediment with identical reaction rates. After the injection of the iron oxide colloidal particles, however, the sediment-associated heavy metals will also adsorb to the pristine iron oxides newly introduced into the aquifer, which likely exhibit a stronger affinity for these metals than the ambient sediment material (see e.g. Montalvo and Smolders (2019)). Furthermore,

injected goethite colloids are deposited on the surface of the sediment particles, placing them in immediate proximity to the sediment-associated heavy metals. This promotes a flux of heavy metals from the sediment to the iron oxides. Consequently, sediment-associated heavy metals may compete with the mobile, dissolved heavy metals from groundwater for adsorption sites on the introduced nanoparticles. Nevertheless, even at the extreme heavy metal content of the sediment at the Nitrastur site, the injected goethite nanoparticles efficiently immobilized the dissolved heavy metal contaminants. For example, in IW5, where high amounts of sediment-associated heavy metals were

present (Fig. 6), the concentrations of dissolved Zn and Cu were reduced from 20 to 30 mg/L to lower than 2 mg/L. Therefore, it is important that both the heavy metal concentration in the groundwater and the content in the sediment must be included in calculating the adsorption capacities of an *in situ* barrier. If the heavy metal content of the sediment is too high, the lifetime of the *in situ* barrier will be significantly reduced. These facts have to be taken into account in evaluating the technical and economic feasibility of the *in situ* adsorption barrier.

Conclusions and environmental implications.

The present study demonstrates the applicability of colloidal goethite nanoparticles for *in situ* immobilization of toxic metals in groundwater. Ca. 1500 kg of humic-acid goethite nanoparticles were injected in 150 m<sup>3</sup> suspension into a contaminated aquifer to form a permeable adsorption barrier of 21 m × 9 m and 3 m thickness. Results of this demonstration study confirmed previous micro- and mesoscale studies that the colloidal goethite nanoparticles are easily injectable in aquifers at low pressures. They follow the pattern of hydraulic conductivity of the sediment, and precipitate within one to two days after the injection, without clogging the pore space. In this way, they form a stable and *in situ* permeable adsorption barrier, which adsorbs and immobilizes dissolved heavy metals from the contaminant plume. Despite the excessive heavy metal concentrations in both sediment and groundwater, the heavy metal concentrations in the groundwater were significantly reduced to less than 50% of the original concentrations after the injection of the goethite nanoparticles. Immobilization of heavy metals was successfully observed both inside the barrier domain and further downstream. The goethite colloids provide an ecologically harmless technology that poses no risk to the environment and to the operators involved. Hence, ferric oxide colloid-based *in situ* adsorption barriers provide a new and competitive option for groundwater remediation.

## Declaration of Competing Interest

The authors declare that they have no known competing financial interests or personal relationships that could have appeared to influence the work reported in this paper.

## Acknowledgement

This work was supported by H2020 EU project “Reground” Grant Agreement N° 641768.

([www.reground-project.eu/](http://www.reground-project.eu/)). The authors gratefully acknowledge the valuable contribution of Sofia Credaro, who assisted in the proof-reading and language editing of the manuscript. The authors thank the constructive comments by two anonymous reviewers.

## Appendix A. Supplementary data

Supplementary data to this article can be found online at <https://doi.org/10.1016/j.jconhyd.2020.103741>.

## References

- Abdus-Salam, N., Adekola, F., 2005. The influence of pH and adsorbent concentration on adsorption of lead and zinc on a natural goethite. *Afr. J. Sci. Technol. (AJST) Sci. Eng. Ser.* 6, 55–66.
- Al-Saad, K.A., et al., 2012. Iron oxide nanoparticles: applicability for heavy metal removal from contaminated water. *Arab J. Nucl. Sci. Appl.* 45 (2), 335–346.
- Baragaño, D., et al., 2020. Arsenic release from pyrite ash waste over an active hydrogeological system and its effects on water quality. *Environ. Sci. Pollut. Res.* 27 (10), 10672–10684.
- Barakat, M.A., 2011. New trends in removing heavy metals from industrial wastewater. *Arab. J. Chem.* 4 (4), 361–377.
- Bianco, C., Patiño Higuera, J.E., Tosco, T., Tiraferri, A., Sethi, R., 2017. Controlled deposition of particles in porous media for effective aquifer nanoremediation. *Sci. Rep.* 7 (1), 12992.
- Braunschweig, J., Bosch, J., Meckenstock, R.U., 2013. Iron oxide nanoparticles in geomicrobiology: from biogeochemistry to bioremediation. *New Biotechnol.* 30 (6), 793–802.
- Cabellos, J., González-Andrés, V., Díez-Ortiz, M., Janer, G.J.T.L., 2018. Iron oxide nanoparticle toxicity on human cell lines, aquatic and soil organisms and interactions with metal pollutants. *Toxicol. Lett.* 295, S209–S210.
- Chuan, M.C., Shu, G.Y., Liu, J.C., 1996. Solubility of heavy metals in a contaminated soil: effects of redox potential and pH. *Water Air Soil Pollut.* 90 (3), 543–556.
- Dolgormaa, A., et al., 2018. Adsorption of Cu (II) and Zn (II) ions from aqueous solution by gel/PVA-modified super-paramagnetic iron oxide nanoparticles. *Molecules* 23 (11), 2982.
- EPA, U., 2009. Nanotechnology for Site Remediation Fact Sheet.
- Fedje, K.K., Sierra, C., Gallego, J.R., 2017. Enhanced soil washing for the remediation of a brownfield polluted by pyrite ash. *Soil Sediment Contam. Int. J.* 26 (4), 377–390.
- Gallego, José Luis Rodríguez, Rodríguez-Valdés, E., Esquinas, N., Fernández-Braña, A., Afif, E., 2016. Insights into a 20-ha multi-contaminated brownfield megasite: An environmental forensics approach. *Science of The Total Environment* 563-564, 683–692. <https://doi.org/10.1016/j.scitotenv.2015.09.153>.
- González-Andrés, V., et al., 2017. Acute ecotoxicity of coated colloidal goethite nanoparticles on *Daphnia magna*: evaluating the influence of exposure approaches. *Sci. Total Environ.* 609, 172–179.
- He, F., Zhao, D., Paul, C., 2010. Field assessment of carboxymethyl cellulose stabilized iron nanoparticles for *in situ* destruction of chlorinated solvents in source zones. *Water Res.* 44 (7), 2360–2370.
- Karn, B., Kuiken, T., Otto, M., 2009. Nanotechnology and *in situ* remediation: a review of the benefits and potential risks. *Environ. Health Perspect.* 117 (12), 1813–1831.
- Khin, M.M., Nair, A.S., Babu, V.J., Murugan, R., Ramakrishna, S., 2012. A review on nanomaterials for environmental remediation. *Energy Environ. Sci.* 5 (8), 8075–8109.
- Kocur, C.M., et al., 2014. Characterization of nZVI mobility in a field scale test. *Environ. Sci. Technol.* 48 (5), 2862–2869.
- Król, A., Mizerna, K., Bozym, M., 2020. An assessment of pH-dependent release and mobility of heavy metals from metallurgical slag. *J. Hazard. Mater.* 384, 121502.
- Marcovecchio, J., Botté, S., Freije, R.H., 2007. Heavy metals, major metals, trace elements. In: Nollé, L. (Ed.), *Handbook of Water Analysis*, 2nd edition. Crc Press, Taylor & Francis Group Lcc, pp. 273–310.
- Meckenstock, R., Bosch, J., 2014. Method for the Degradation of Pollutants in Water and/or Soil (Google Patents).
- Mehra, O.P., Jackson, M.L., 1958. Iron oxide removal from soils and clays by a dithionite-citrate system buffered with sodium bicarbonate. *Clay Clay Miner.* 7 (1), 317–327.
- Mohapatra, M., Mohapatra, L., Singh, P., Anand, S., Mishra, B.K., 2010. A comparative study on Pb(II), Cd(II), Cu(II), Co(II) adsorption from single and binary aqueous solutions on additive assisted nano-structured goethite. *Int. J. Eng. Sci. Technol.* 2 (8), 89–103.
- Montalvo, D., Smolders, E., 2019. Metals and metalloid removal by colloidal humic acid-Goethite: column experiments and geochemical modeling. *Vadose Zone J.* 18 (1), 1–9.
- Montalvo, D., Vanderschueren, R., Fritzsche, A., Meckenstock, R.U., Smolders, E., 2018. Efficient removal of arsenate from oxic contaminated water by colloidal humic acid-coated goethite: batch and column experiments. *J. Clean. Prod.* 189, 510–518.
- Okazaki, M., Takamidoh, K., Yamane, I., 1986. Adsorption of heavy metal cations on hydrated oxides and oxides of iron and aluminum with different crystallinities. *Soil Sci. Plant Nutr.* 32 (4), 523–533.
- Paya Perez, A., Rodríguez Eugenio, N., 2018. Status of Local Soil Contamination in Europe: Revision of the Indicator “Progress in the Management Contaminated Sites in Europe”. Publications Office of the European Union (ISSN: 1831-9424).
- Perelo, L.W., 2010. Review: *in situ* and bioremediation of organic pollutants in aquatic sediments. *J. Hazard. Mater.* 177 (1), 81–89.
- Phenrat, T., Saleh, N., Sirk, K., Tilton, R.D., Lowry, G.V., 2007. Aggregation and sedimentation of aqueous nanoscale zerovalent iron dispersions. *Environ. Sci. Technol.* 41 (1), 284–290.
- Rodda, D.P., Johnson, B.B., Wells, J.D., 1993. The effect of temperature and pH on the adsorption of copper(ii), lead(ii), and zinc(ii) onto goethite. *J. Colloid Interface Sci.* 161 (1), 57–62.
- Saha, I., et al., 2013. Role of nanotechnology in water treatment and purification: potential applications and implications. *Int. J. Chem. Sci. Technol.* 3 (3), 59–64.
- Saleh, N., et al., 2006. Surface modifications enhance nanoiron transport and napl targeting in saturated porous media. *Environ. Eng. Sci.* 24 (1), 45–57.
- Schwertmann, U., 1991. Solubility and dissolution of iron oxides. *Plant Soil* 130 (1), 1–25.
- Shen, Q., Demisie, W., Zhang, S., Zhang, M., 2020. The association of heavy metals with iron oxides in the aggregates of naturally enriched soil. *Bull. Environ. Contam. Toxicol.* 104 (1), 144–148.
- Skjolding, L.M., et al., 2016. Aquatic ecotoxicity testing of nanoparticles—the quest to disclose. *Nanopart. Effects* 55 (49), 15224–15239.
- Tiraferri, A., Chen, K.L., Sethi, R., Elimelech, M., 2008. Reduced aggregation and sedimentation of zero-valent iron nanoparticles in the presence of guar gum. *J. Colloid Interface Sci.* 324 (1), 71–79.
- Tiraferri, A., Saldarriaga Hernandez, L.A., Bianco, C., Tosco, T., Sethi, R., 2017. Colloidal behavior of goethite nanoparticles modified with humic acid and implications for aquifer reclamation. *J. Nanopart. Res.* 19 (3), 107.
- Tosco, T., Bosch, J., Meckenstock, R.U., Sethi, R., 2012. Transport of ferrihydrite nanoparticles in saturated porous media: role of ionic strength and flow rate. *Environ. Sci. Technol.* 46 (7), 4008–4015.

- Tosco, T., Petrangeli Papini, M., Cruz Viggi, C., Sethi, R., 2014. Nanoscale zerovalent iron particles for groundwater remediation: a review. *J. Clean. Prod.* 77, 10–21.
- Uwamariya, V., 2013. Adsorptive Removal of Heavy Metals from Groundwater by Iron Oxide Based Adsorbents. IHE Delft Institute for Water Education, ISBN 1138020648.
- Velimirovic, M., Carlo, B., Ferrantello, N., Tosco, T., Casasso, A., Sethi, R., Schmid, D., Wagner, S., Miyajima, K., Klaas, N., Meckenstock, R.U., von der Kammer, F., Hofmann, T., 2020. A large-scale 3d study on transport of humic acid-coated goethite nanoparticles for aquifer remediation. *Water* 12 (4), 1207.
- Vermeer, A.W.P., McCulloch, J.K., van Riemsdijk, W.H., Koopal, L.K., 1999. Metal ion adsorption to complexes of humic acid and metal oxides: deviations from the additivity rule. *Environ. Sci. Technol.* 33 (21), 3892–3897.
- Violante, A., Cozzolino, V., Perelomov, L., Caporale, A.G., Pigna, M., 2010. Mobility and bioavailability of heavy metals and metalloids in soil environments. *J. Soil Sci. Plant Nutr.* 10, 268–292.
- Waychunas, G.A., Kim, C.S., Banfield, J.F., 2005. Nanoparticulate iron oxide minerals in soils and sediments: unique properties and contaminant scavenging mechanisms. *J. Nanopart. Res.* 7 (4), 409–433.
- Wcislo, E., Bronder, J., Bubak, A., Rodríguez-Valdés, E., Gallego, J.L.R., 2016. Human health risk assessment in restoring safe and productive use of abandoned contaminated sites. *Environ. Int.* 94, 436–448.